Design of Compact Stacked-Patch Antennas in LTCC multilayer packaging modules for Wireless Applications

R. L. Li, G. DeJean, K. Lim, M. M. Tentzeris, and J. Laskar

School of Electrical and Computer Engineering
Georgia Institute of Technology
Atlanta, GA 30332-250, U.S.A.
E-mail: rlli@ece.gatech.edu
Phone: 404-894-3360
Fax: 404-894-4641

Abstract— A simple procedure for the design of compact stacked-patch antennas is presented based on LTCC multilayer packaging technology. The advantage of this topology is that only one parameter, i.e., the substrate thickness (or equivalently the number of LTCC layers), needs to be adjusted in order to achieve an optimized bandwidth performance. The validity of the new design strategy is verified through applying it to practical compact antenna design for several wireless communication bands, including ISM 2.4 GHz band, IEEE 802.11a 5.8 GHz, and LMDS 28 GHz band. It is shown that a 10-dB return-loss bandwidth of 7% can be achieved for the LTCC (ε_r=5.6) multilayer structure with a thickness of less than 0.03 wavelengths, which can be realized using a different number of laminated layers for different frequencies (e.g. 3 layers for the 28 GHz band)

Index terms— Compact antennas, LTCC packages, wireless communications, multilayer RF modules, embedded antennas.

I. Introduction

The explosive growth of wireless communications systems has led to an increasing demand for integrated compact low-cost antennas. It is well known that the large size of most planar antennas is one of the major limiting factors for the miniaturization of RF devices and leads to System-on-Package (SOP) solutions with externally integrated antennas. Lately, the LTCC (Low Temperature Co-fired Ceramics) multilayer packaging technology is becoming more and more popular for the production of highly integrated, complex multilayer RF modules [1]. This technology is appreciated for its flexibility in realizing an arbitrary number of layers, something that allows for the easy and highly compact vertical integration of wireless transceivers. Recently a 3-dimensional LTCC multilayer module was proposed for compact RF front-end, which is integrated with a patch antenna [2]. However, the integrated patch antenna had a narrow bandwidth due to the high dielectric constant of the LTCC packaging materials, thus making it difficult to meet the bandwidth requirement for some broadband wireless communication systems.

A common approach for improving the bandwidth performance of a patch antenna is to add parasitic elements to the antenna structure, e.g., a stacked patch [3]. This reduces the impedance variation of the antenna with frequency, thus enhancing bandwidth performance. Various arrangements of stacked structures have been investigated in [4]-[5]. Typically a stacked configuration of layers with foam and low dielectric constant or a combination of high and low dielectric constant material is used to achieve a broad bandwidth. These structures require a thicker substrate (typically the total antenna thickness=~$0.1\lambda_0$, λ_0=wavelength in free space) and

different materials. This approach is not suitable for the LTCC packages with demanding compactness requirements. In addition, the design of such a different-substrate-stacked patch antenna is often a very tedious procedure. There are many parameters that need to be adjusted for an optimized bandwidth performance, such as the length and width of each patch, the thickness of each substrate, as well as the position of the feed point. In practice it is very difficult to adjust every parameter for optimal performance.

In this paper, a simple design method is presented for compact stacked-patch antennas based on LTCC multilayer structures. It is found that an optimal bandwidth performance can be always obtained by modifying only the number of the LTCC layers. First, the design methodology is investigated for LTCC layers with different dielectric constants. It is found that the broadband performance (with VSWR<2) can be achieved for the dielectric constant ε_r =3 to 7. This design procedure is then applied to LTCC Kyocera-GL550 substrate (ε_r =5.6) for three wireless communication bands. It is shown that the stacked-patch antennas on such an LTCC multilayer substrate can double the impedance bandwidth, as compared to a single-patch antenna with the same substrate, while maintaining a thin dielectric substrate.

II. Antenna Structure and Design Strategy

The antenna structure considered throughout this paper is shown in Fig. 1, where the patch antenna is integrated with a 3-D RF frond-end module in an LTCC multilayer package. To simplify the design procedure, the two patches (lower and upper) are assumed to be square with the same dimensions and to be stacked on a grounded

LTCC multilayer substrate that has a total thickness of h. The lower patch divides the LTCC substrate into a lower (thickness=h_1) and an upper part (thickness =h_2). The stacked patch is backed by a metal cavity, while the lower patch is fed through a probe extended from a 50Ω coaxial line.

In modern RF front-end modules, it is highly desirable to integrate the antenna with other RF circuits. Therefore, it is essential to prevent any unwanted radiation from other RF components in the integrated chip. For this reason, we introduce a metal-backed cavity in order to shield the RF signals generated inside the transceiver from the antenna signals. In LTCC packaging technology, the sidewall of the metal cavity can be easily realized through an array of vertical vias in order to minimize the losses at the cavity's metal walls. We select the lateral dimension of the cavity to be twice of that of the stacked patch in order to reduce the reflection from the sidewall, which may affect the impedance characteristics of the antenna. To simplify the design procedure, we fix the position of the feed probe to the center of the edge of the lower patch in order to match with a 50Ω coaxial line.

The wide-bandwidth performance of the stacked-patch antenna is achieved due to a combination of two close resonant frequencies which respond respectively to the lower patch and the upper patch. The combination is made by an electromagnetic coupling between the two patch resonators, which can be modeled by the equivalent circuit shown in Fig. 2. This circuit consists of two electromagnetically coupled (C=coupling capacitance and M=mutual inductance) parallel resonant circuits (R_1, R_2 =radiation resistance, L_1, L_2 and C_1, C_2=equivalent inductance and capacitance respectively associated with the lower and upper patch resonators) and a series

inductor (inductance=L_p) to model the inductance of the feed probe. Two resonant frequencies depends on L_1C_1 and L_2C_2 while the tightness of the electromagnetic coupling is decided by the coupling capacitance C and mutual inductance M. Through an adjustment of the heights of the lower and lower patches, we can change their resonant frequencies and the coupling tightness, thus resulting in an optimal impedance performance.

To further understand the design philosophy, we numerically investigate the input impedance characteristics of the stacked-patch antenna on the LTCC substrate for different dielectric constants. Fig. 3 shows the simulated (using Micro-Stripes 5.6) input impedance loci on a Smith chart for ε_r =2, 4, 6, 8, 10. It can be seen that there always exists a loop in the impedance locus (resulting from the electromagnetic coupling between the two stacked patches). The size of the loop decreases with an increase in the dielectric constant, because the coupling between the two patches becomes tight. Also, when the dielectric constant increases, the impedance locus shifts toward the lower side of the Smith chart due to the increased capacitive coupling. In order to move the loop toward the center of the Smith chart, we need to change the coupling between the two patches by adjusting their relative position, i.e., h_1 or h_2. Usually the total thickness (h_1+h_2) of the antenna is fixed for a certain bandwidth requirement and most of the times wider bandwidths demand thicker substrates. Therefore, we only need to adjust h_1. For a higher dielectric constant, h_1 should decrease to loosen the coupling. Fig. 4 demonstrates the variation of the loop position with h_1. It is shown that the impedance loops can be adjusted to situate inside the VSWR=2 circle when h_1=1, 0.6, and 0.5 mm respectively for ε_r =3, 5, and 7.

Based on the above analysis, we investigated the impedance performance of the stacked-patch antennas on LTCC Kyocera-GL550 multilayer substrate with layer thickness =4 mils, dielectric constant ε_r = 5.6, and loss tangent=0.0012. Following numerous numerical simulations, we found the relationship between the bandwidth and substrate thickness for a compact substrate (thickness=0.01-0.03λ_0), which is shown in Fig. 5, where the relative 10-dB return-loss bandwidth (normalized to the center frequency f_c) is plotted as a function of the thickness (normalized to the free-space wavelength λ_0 at f_c). For comparison, the bandwidth of a single-patch antenna with the same type of substrate is also presented in this figure. It is observed that the compact stacked-patch antenna can achieve a bandwidth of up to 7%, 60%-70% wider than a single-patch antenna could. For convenience in applications, we now summarize the basic steps for the stacked-patch antenna design as follows.

Step 1: Select the preliminary total thickness h ($=h_1+h_2$) of substrate according to the bandwidth requirement for a specific application.

Step 2: Select the thickness of lower substrate h_1. We have found through numerous simulations that for the LTCC GL550 substrate the resonant loop appears near the center of the Smith chart when the ratio of the lower-substrate thickness to that of the upper substrate is around 1:3. Therefore, we can choose $h_1=h/4$.

Step 3: Perform a preliminary design, choosing the length of the stacked patch L according to the specified center frequency for a practical application. For convenience, we suggest making use of the typical approximate equation: $L = 1/(2f_c\sqrt{\mu_0\varepsilon_0\varepsilon_r})$ [3].

Step 4: Determine the upper-substrate thickness h_2 for an optimal return loss. The initial value of h_2 can be chosen as $3h_1$ according to Step 2. The final value of h_2 may be obtained by numerical simulation. Upon our observation, it is found that the resonant loop in the Smith chart will move from the upper Smith chart (inductive) to the lower (capacitive) as the upper patch moves toward the lower patch. h_2 is determined when the center of the resonant loop moves most close to the center of the Smith chart, which corresponds to a minimum return loss. Based on numerical and experimental analysis, the value of h_2 should be $2h_1<h_2<4h_1$.

Step 5: Adjust L to a final value that enables the bandwidth to fully cover the specified band of the practical specification. This also can be carried out with the help of numerical simulation.

If the final optimized bandwidth does not meet the requirement for the specified band, h_1 has to increase slightly and Steps 4 and 5 have to be repeated until the specification is satisfied.

III. Applications

In this section the design principles described above are applied to the antenna design for three wireless communication bands: ISM (Industrial Scientific and Medical) 2.4 GHz band (2.4-2.483 GHz) [6], IEEE 802.11a 5.8 GHz ISM band (5.725-5.85 GHz) [7], and LMDS 28 GHz band (27.5-29.25 GHz) [8].

A. ISM 2.4 GHz Band

According to the band specification, the relative bandwidth is calculated to be 3.4%. Looking up Fig. 5, we find the total thickness of substrate to be about $0.015\lambda_0$. The central design frequency, f_c , of this band is 2.4415 GHz, resulting in a physical thickness of the substrate equal to 1.84 mm, which is approximately equal to 18 LTCC layers. Considering that the lower-substrate thickness should be roughly a quarter of the total substrate thickness, we choose $h_1=5$ layers. Substituting f_c=2.4415 GHz into $L = 1/(2f_c\sqrt{\mu_0\varepsilon_0\varepsilon_r})$, we get $L=1022$ mils. Then, the upper-substrate thickness h_2 can be determined through numerical experiments for values between $2h_1<h_2<4h_1$. The simulated input impedance is plotted for different h_2 (in layers) in a Smith chart as illustrated in Fig. 6. It can be observed that the resonant loop does move from the upper to lower half of the Smith chart as h_2 reduces. The optimal bandwidth performance is obtained when the resonant loop is completely located inside the VSWR=2 circle. We find $h_2=14$ layers which is very close to 13 layers, the initial value of h_2. The last design step involves the adjustment of L in order for the antenna to meet the band specification. Upon simulation, L needs to be reduced to $L=966$ mils. The final result for the impedance characteristic is depicted in Fig. 7.

B. IEEE 802.11a 5.8 GHz band

Following a similar procedure , we initially choose $h_1=2$ layers, $h_2= 6$ layers, and L=400 mils. The input impedance locus in the Smith chart is shown in Fig. 8 for different h_2. Coincidentally, it is found that the optimized h_2 (also 6 layers) is exactly equal to the initial value. This antenna was fabricated by Kyocera Ceramics. Fig. 9

shows the simulated and measured results for return loss and good agreement is observed. We can also see that the bandwidth of the stacked-patch antenna is much broader than the required band. That means that the antenna thickness can be further reduced if we could change h_1 continuously instead of consecutively or if, equivalently, LTCC layers of variable thickness can be utilized in the module fabrication.

C. LMDS 28 GHz Band

Even though the LMDS is a broadband application (7% bandwidth), we only need to choose $h_1=1$ layer due to its high center frequency. From Fig. 5, the total thickness can be found to be about 0.03 wavelengths, which approximately correspond to a physical size of 0.32 mm, about 3 LTCC layers. As we mentioned in Step 2 of the design procedure, h_1 should be roughly a quarter of the total thickness. This means that h_1 needs to be only 0.8 layers, rounded to one layer. The effect of h_2 on the impedance performance has to be carefully accessed and the simulated results are shown in Fig. 10. It is noted that the optimal bandwidth is achieved when $h_2=2$ layers. The length of the stacked patch is found to be $L=80$ mils to cover the specified band. The performance of the LTCC antenna topology is shown in Fig. 11. To demonstrate the validity of the simulated result, the return loss calculated by using FDTD is also presented in this figure, demonstrating a very good agreement for the frequency band of the antenna design.

The radiation pattern of the stacked-patch antenna is very similar to that for a typical single-patch antenna. Fig. 12 shows a pattern comparison between stacked-

and single-patch antennas for the same thickness (h_1+h_2). We can see that the co-polarized components are completely same while the cross-polarized component for the stacked patch is about 10 dB lower than that for the single patch due to a much shorter fed probe for the stacked patch. It has to be noted that the feed probe for the single patch is ~4 times longer ((h1+h2) instead of (h1)) than that for the stacked patch. Also, the radiation efficiency for both antennas is higher than 95%. It can be easily demonstrated by theoretical analysis that the radiation efficiency is dependent on the resonant frequency, the dielectric constant and the height of substrate. In general, the efficiency increases with the thickness of the substrate and decreases with increasing dielectric constant. From Fig. 5 we can see that in order to achieve the same bandwidth, the thickness for a single-patch may need to be doubled in comparison to the stacked-patch antenna, which would constitute one of the best and more compact solutions for multilayer (LTCC, MLO) wireless transceivers.

IV. Conclusion

A simple procedure for the design of compact stacked-patch antennas has been presented based on LTCC multilayer packaging technology. The advantage of this topology is that only one parameter, i.e., the substrate thickness (or equivalently the number of LTCC layers), needs to be adjusted in order to achieve an optimized bandwidth performance. This approach is suitable for the design of compact broadband antennas that can be easily integrated with vertically integrated transceivers and facilitate the system-level packaging. It is demonstrated that a stacked-patch antenna on an LTCC substrate with a thickness of less than $0.03\lambda_0$ can

achieve a bandwidth of up to 7%, which may find applications in a number of wireless communication systems up to the millimeter frequency range (WLAN 802.11x, LMDS).

Acknowledgement

The authors wish to acknowledge the support of Yamacraw Design Center of the State of Georgia, the NSF Career Award under contract NSF #9964761, and the NSF Packaging Research Center of Georgia Tech.

References

[1] B. Hunt and L. Devlin, "LTCC for RF modules," *Packaging and Interconnects at Microwave and mm-Wave Frequencies IEE Seminar*, pp. 5/1-5/5, 2000

[2] K. Lim, S. Pinel, M. Davis, A. Sutono, C.-H. Lee; D. Heo, A. Obatoynbo, J. Laskar, E. M. Tantzeris, and R. Tummala, "RF-system-on-package (SOP) for wireless communications," *IEEE Microwave Magazine*, vol. 3, no. 1, pp. 88–99, 2002.

[3] P. Bhartia, Inder. Bahi, R. Garg, and A. Ittipiboon, *Microstrip Antenna Design Book*, Artech House, 2000.

[4] R. B. Waterhouse, "Design of probe-fed stacked patches," *IEEE Trans. Antennas Propagat*., vol. 47, no. 12, pp. 1780-1784, 1999.

[5] R. B. Waterhouse, "Stacked patches using high and low dielectric constant material combinations," *IEEE Trans. Antennas Propagat*., vol. 47, no.12, pp. 1767-1771, 1999.

[6] J. C. Haartsen, “The Bluetooth radio system,” *IEEE Personal communications*, vol. 7, no.1, pp. 28-36, 2000.

[7] *IEEE 802.11, IEEE Standard for Wireless LAN Medium Access Control and Physical Layer Specifications*, 1999.

[8] A. Nordbotten, “LMDS systems and their applications,” *IEEE Communications Magazine*, vol. 38, no. 6, pp. 150-154, 2000.

List of Figure Captions

Fig. 1. Stacked-patch antenna in a LTCC multilayer package.

Fig. 2. Equivalent circuit of the probe-fed stacked-patch antenna.

Fig. 3. Input impedance loci of a stacked-patch antenna on different dielectric constants (L=10 mm, h_1=h_2=1 mm).

Fig. 4. Adjustment of input impedance loci of a stacked-patch antenna on different dielectric constants (L=10 mm, h=2 mm).

(a) ε_r=3
(b) ε_r=5
(c) ε_r=7

Fig. 5. Relationship between the impedance bandwidth and total thickness of patch antennas on LTCC GL550 substrate.

Fig. 6. Input impedance loci of a stacked-patch antenna for ISM 2.4 GHz band.

Fig. 7. Optimal input impedance characteristics of a stacked-patch antenna for ISM 2.4 GHz band (h_2=14).

Fig. 8. Input impedance loci of a stacked-patch antenna for IEEE 802.11a 5.8 GHz band.

Fig. 9. Simulated and measured results for return loss of a stacked-patch antenna for IEEE 802.11a 5.8 GHz band (h_2=6).

Fig. 10. Input impedance loci of a stacked-patch antenna for LMDS 28 GHz band.

Fig. 11. Optimal input impedance characteristics of a stacked-patch antenna for LMDS 28 GHz band (h_2=2).

Fig. 12. Pattern comparison of stacked- and single-patch antennas for LMDS band at 28 GHz.

(a) co-polarized component
(b) cross-polarized component

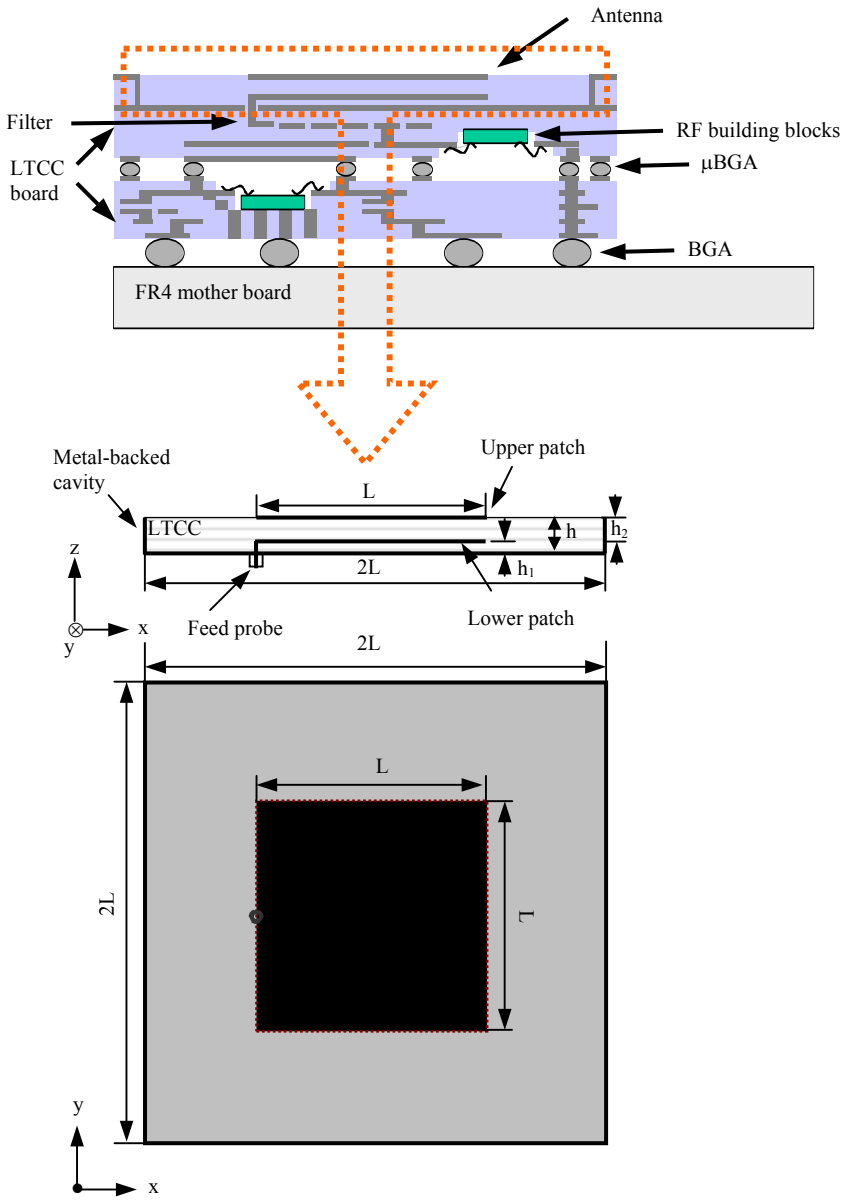

Fig. 1. Stacked-patch antenna in an LTCC multilayer package.

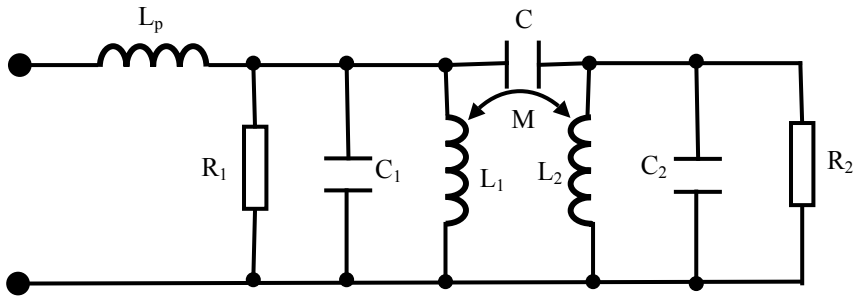

Fig. 2. Equivalent circuit of the probe-fed stacked-patch antenna.

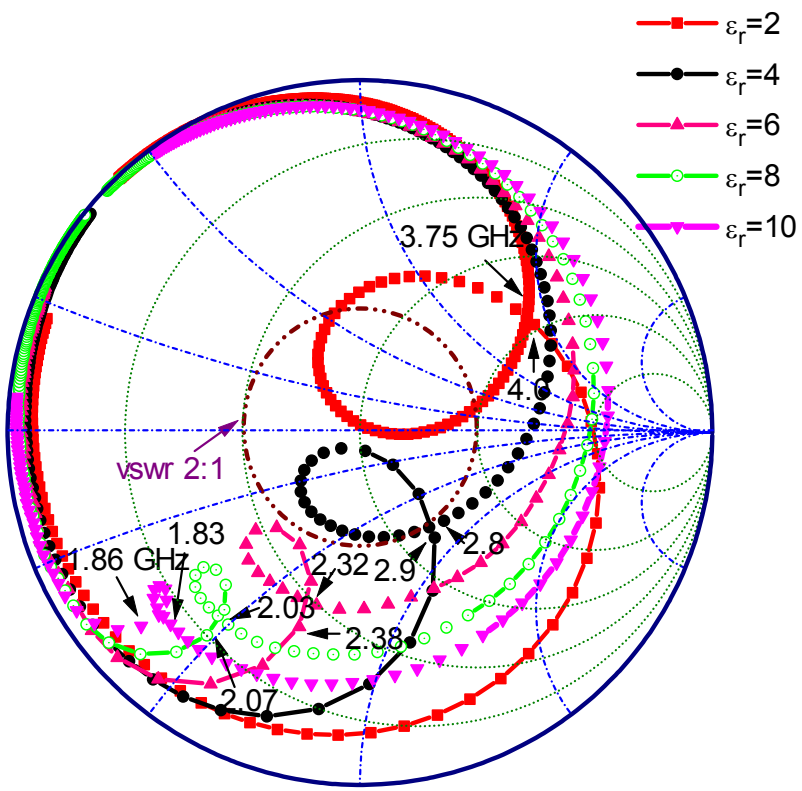

Fig. 3. Input impedance loci of a stacked-patch antenna on different dielectric constants (L=10 mm, h_1=h_2=1 mm).

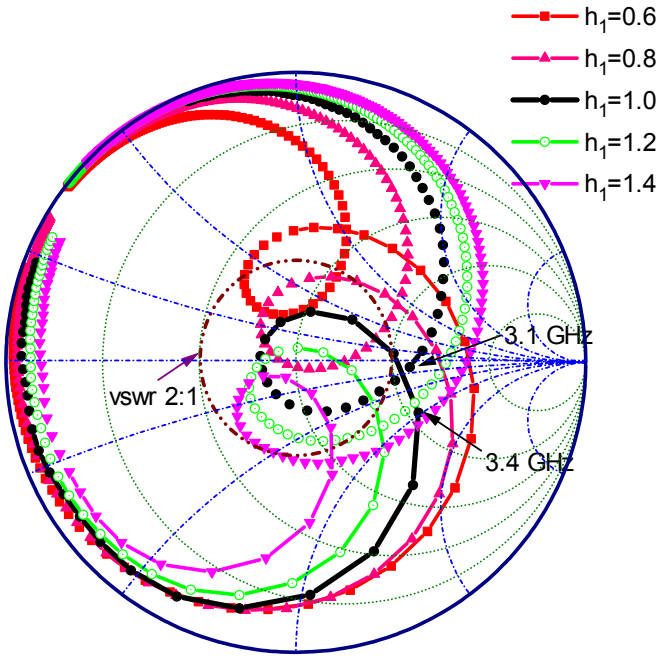

(a) ε_r=3

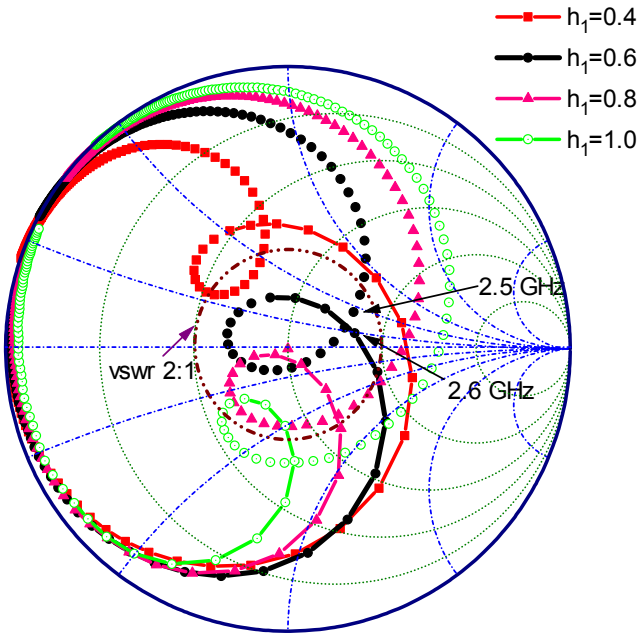

(b) ε_r=5

Fig. 4. Adjustment of input impedance loci of a stacked-patch antenna on different dielectric constants (L=10 mm, h=2 mm).

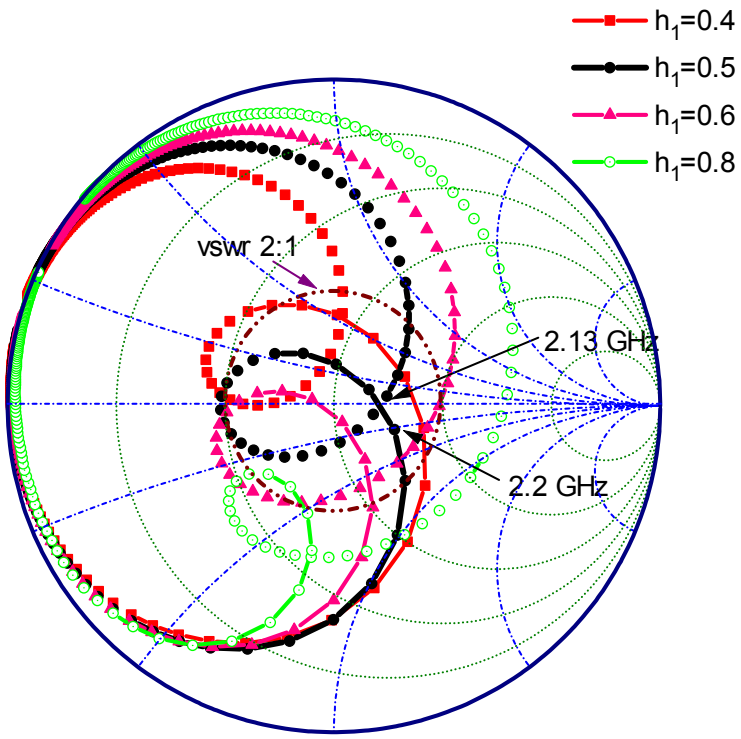

(c) ε_r=7

.

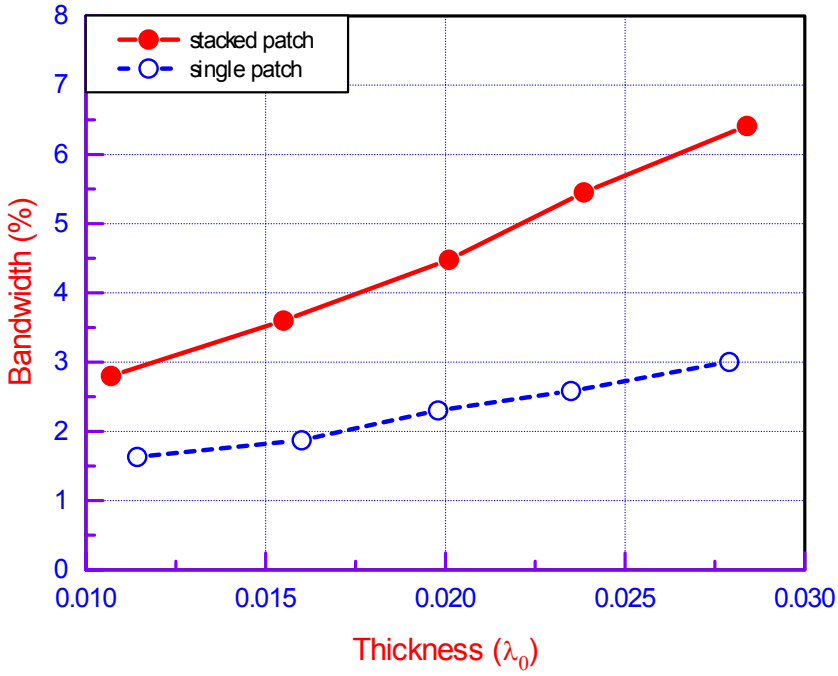

Fig. 5. Relationship between the impedance bandwidth and total thickness of patch antennas on LTCC GL550 substrate.

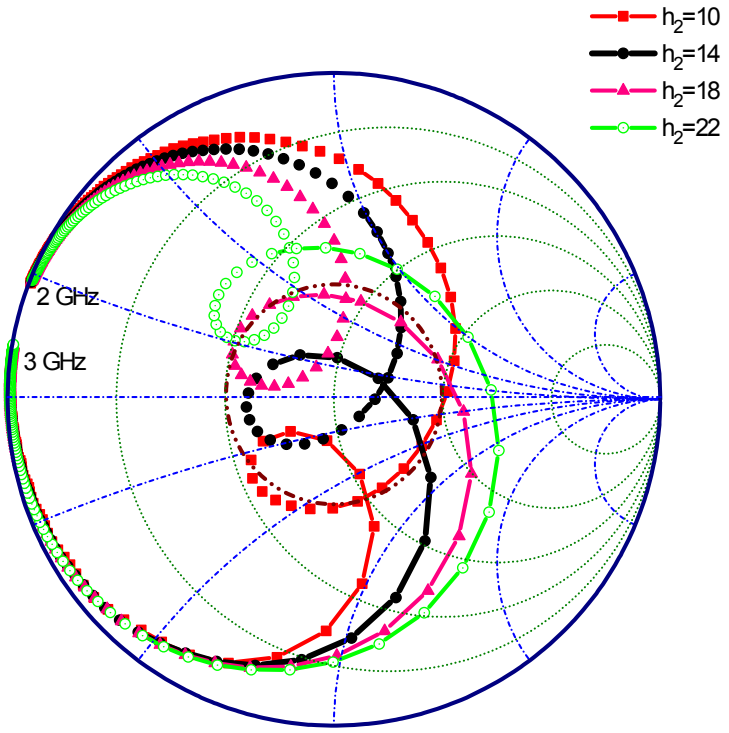

Fig. 6. Input impedance loci of a stacked-patch antenna for ISM 2.4 GHz band.

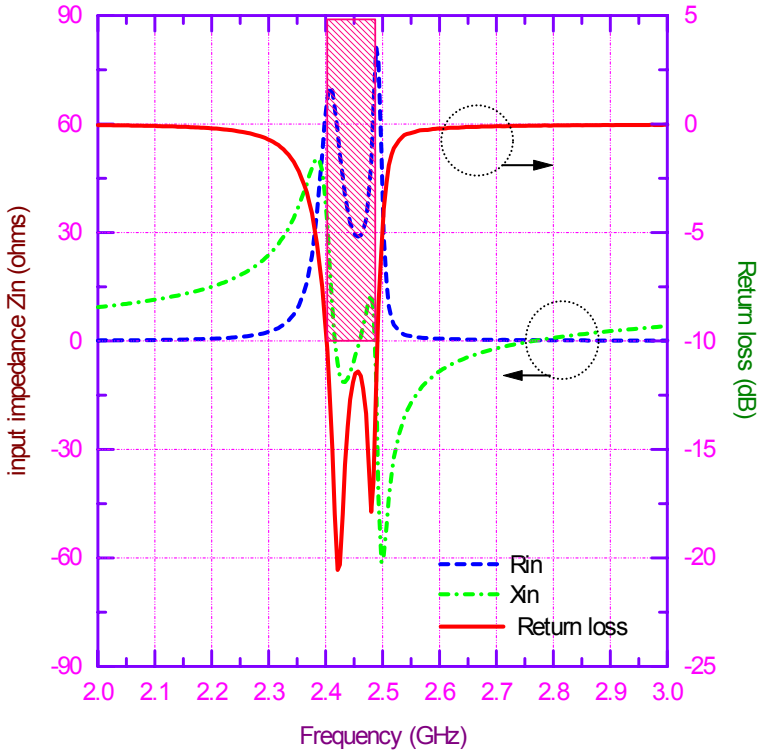

Fig. 7. Optimal input impedance characteristics of a stacked-patch antenna for ISM 2.4 GHz band (h_2=14).

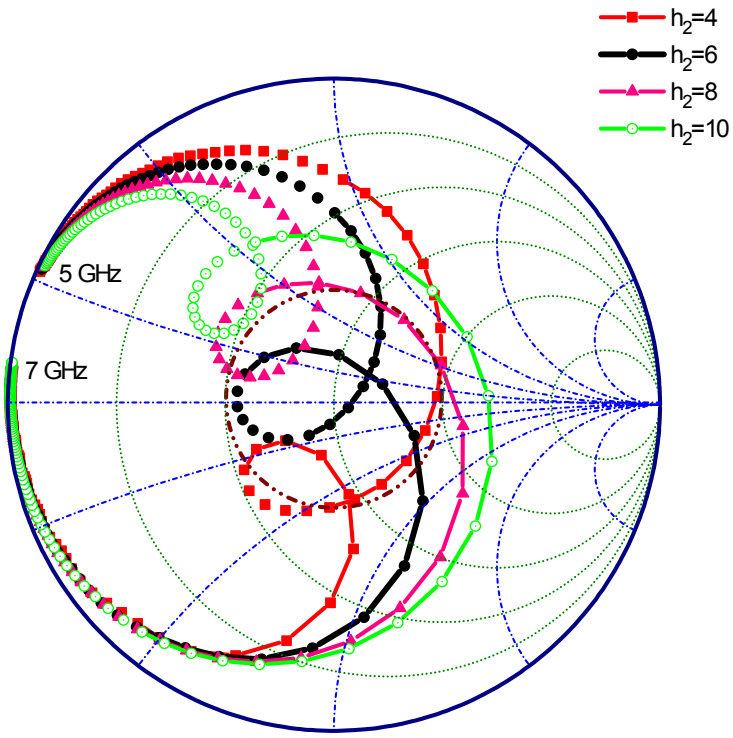

Fig. 8. Input impedance loci of a stacked-patch antenna for IEEE 802.11a 5.8 GHz band.

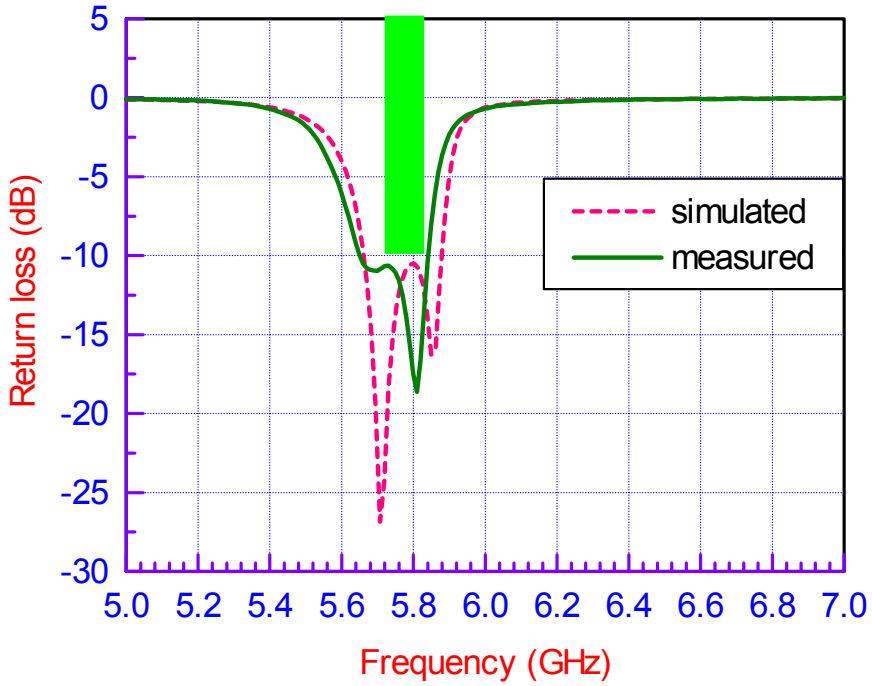

Fig. 9. Simulated and measured results for return loss of a stacked-patch antenna for IEEE 802.11a 5.8 GHz band (h_2=6).

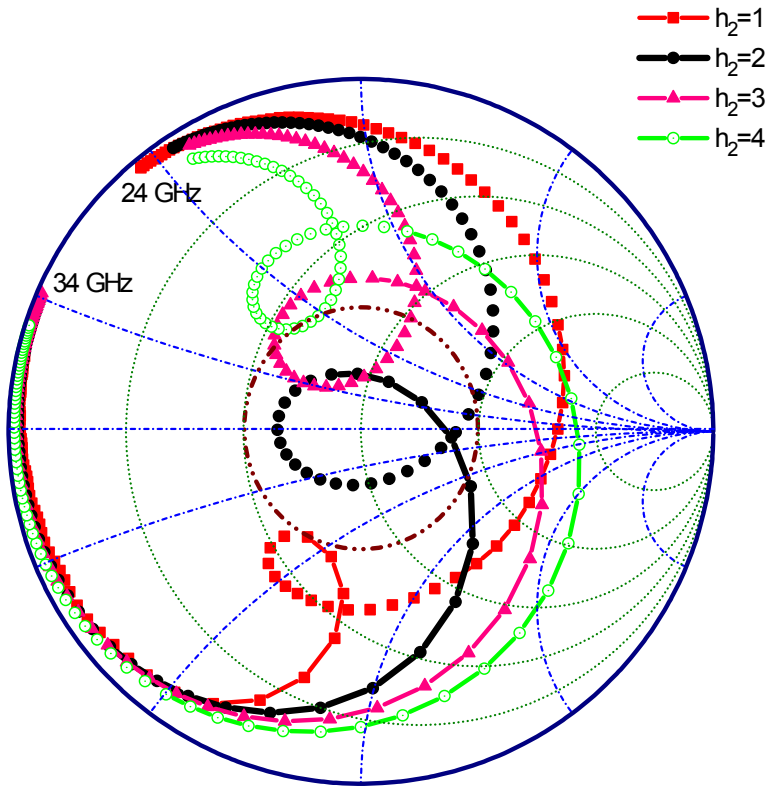

Fig. 10. Input impedance loci of a stacked-patch antenna for LMDS 28 GHz band.

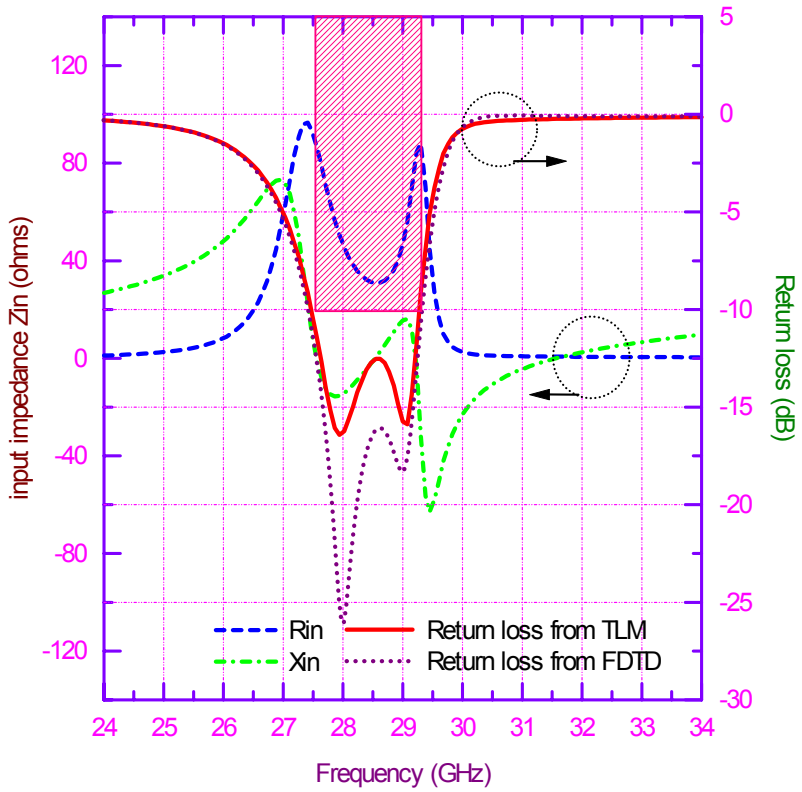

Fig. 11. Optimal input impedance characteristics of a stacked-patch antenna for LMDS 28 GHz band (h_2=2).

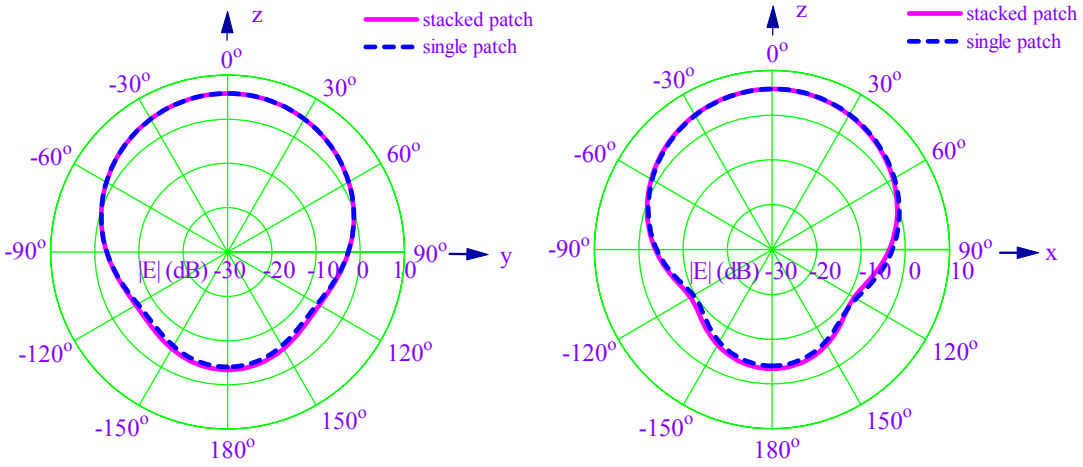

(a) co-polarized component

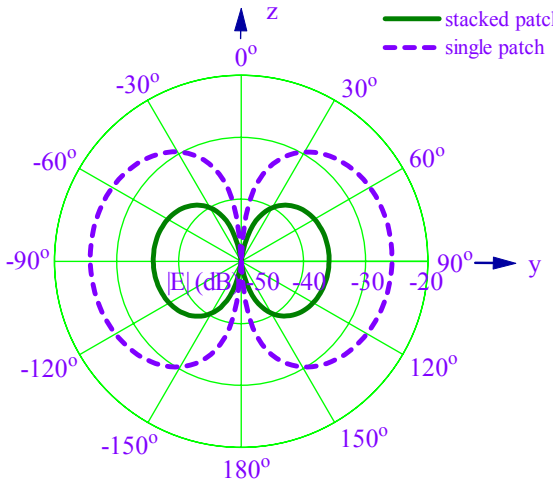

(b) cross-polarized component

Fig. 12. Pattern comparison of stacked- and single-patch antennas for LMDS band at 28 GHz.